Supplementary Information

Strategies for improving the stability, selectivity, and cell voltage of a bipolar membrane zero-gap electrolyzer for low-loss CO_2 reduction

Bhavin Siritanaratkul, Preetam K. Sharma, Eileen H. Yu, Alexander J. Cowan*

1 Stephenson Institute for Renewable Energy and the Department of Chemistry, University of Liverpool, Liverpool, L69 7ZF, UK

2 Department of Chemical Engineering, Loughborough University, Loughborough, LE11 3TU, UK

Table S1. Performance of reverse-bias bipolar membrane cells for CO production from the literature

Reference	Cathode	Anode	Membrane	Anolyte	Current Density (mA cm^{-2})	Cell Voltage (V)	CO FE (%)
2022 Siritanaratkul[1]	Ag	RuO_2	Fumasep FBM	H_2O	25	3.8	17
					100	5.0	22
	Ni[Cyc]$^{2+}$	RuO_2	Fumasep FBM	H_2O	25	3.8	63
					100	4.9	23
	Ni[CycCOOH]$^{2+}$	RuO_2	Fumasep FBM	H_2O	25	3.7	44
					100	4.7	33
2022 Blommaert[2]	Ag	Ni foam	Fumasep FBM	1 M KOH	100	3.7	30
					300	4.8	11
2022 Xie[3]	Ag	IrO_2/Ti	Fumasep FBM	3 M KOH	100	-	46
					200	-	34
2021 Yang[4]	Ag	Ni foam	Fumasep FBM	0.2 M KOH	100	3.7	20
					200	4.3	16
				1 M KOH	100	3.7	41
					200	4.4	32
				3 M KOH	100	4	59
					200	4.9	48
2021 Yan[5]	Ag	Pt	Layer-by-layer BPM	1 M KOH	20	3.4	43
					75	3.7	29
			Nafion BPM	1 M KOH	20	3.4	7
					75	3.7	5
2018 Salvatore[6]	Ag	Ni foam	Fumasep FBM	1 M NaOH	20	-	25
					100	-	8
	Ag (with buffer layer)	Ni foam	Fumasep FBM	1 M NaOH	20	-	78
					100	-	67
					200	-	44

Linear sweep voltammetry of CoPc/carbon compared to blank carbon

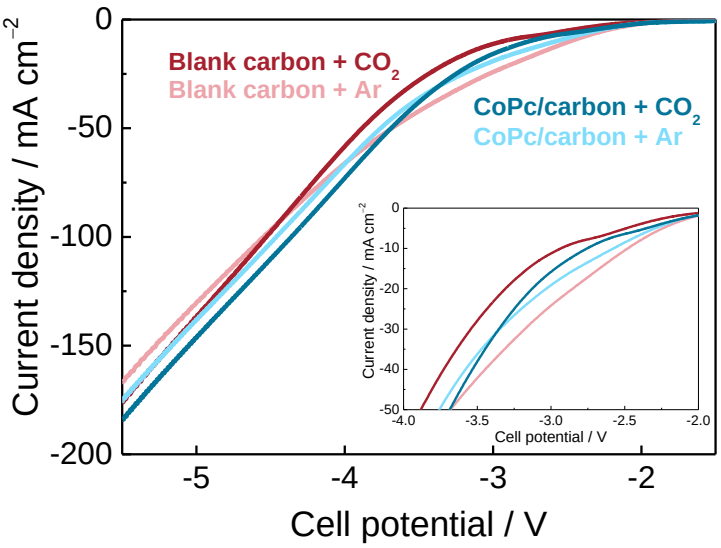

Figure S1. Linear sweep voltammograms of CoPc/carbon in CO_2 (dark blue), Ar (light blue), and blank carbon in CO_2 (dark red), Ar (light red). The inset shows a magnification of the current onset region. Conditions: scan rate 10 mV s^{-1}, swept from -1.5 to -5-5 V, anode RuO_2, anolyte pure water, membrane Fumasep FBM, room temperature.

Electroactive coverage

A **B**

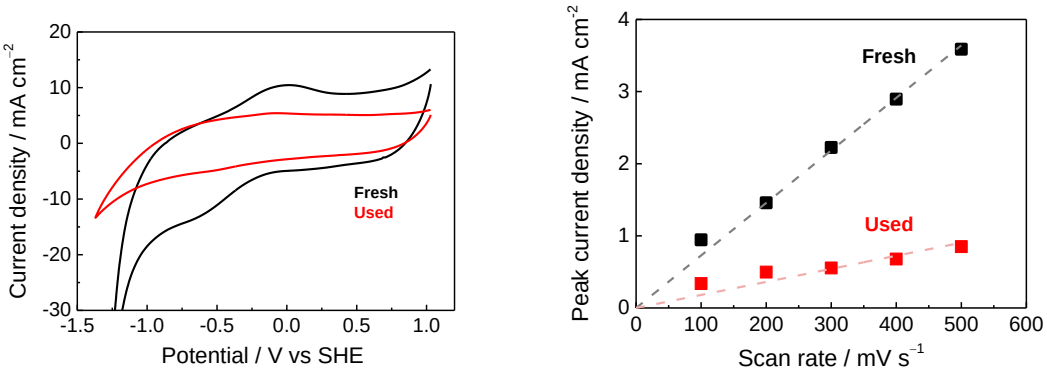

Figure S2. Electroactive coverage of CoPc/carbon cathode. A) Cyclic voltammograms at 500 mV s^{-1} B) scan rate dependence of the oxidative peak at ~0.25 V vs SHE. Conditions: Electrolyte 0.1 M $KHCO_3$, Reference electrode Ag/AgCl, Counter electrode Pt wire, Ar purged.

C 1s and N 1s X-ray Photoelectron Spectroscopy (XPS)

As shown in Figure S3A, peaks at 285.0, 286.0, 286.9, 288.1, 289.8 and 292.4 eV which were assigned to various chemical species were found. The peak at 285.0 eV correspond to C-C/C-H coming from the adventitious carbon which is present in all the samples. The peak at 286.0 corresponds to carbon present in the aromatic rings of CoPc.[7] The peak at 286.9 eV is assigned to the carbon connected to nitrogen atoms and aromatic rings. The peaks at 288.1 and 289.8 eV were showing the satellite contributions. There may be minor contributions from the adventitious carbon to the other peaks. Also, because of the complex nature of the catalyst surfaces, in fresh, used-short and used-long samples, there are some contributions from Nafion binder and carbon powder which could not be resolved. Part of the contribution of Nafion binder can be seen by the presence of C-F peak in GDE samples.[1] The peaks were normalised to the peak at 285.0 eV, the lower intensity of other peaks in case of GDE samples as compared to powder, indicates the presence of other components on the surface along with catalyst on the GDE surface.

N 1s spectra from various samples show peaks at 399.5, 400.0, 401.5 and 402.6 eV (Figure S3B). The peaks at 399.5 and 400.0 are present in the powder CoPc sample also indicating that the peaks should be coming from CoPc structure. Based on the CoPc structure, the peak at 399.5 eV was assigned to nitrogen bound to Co centre and N bridging the 4 organic units of the structure.[7] The peak at 401.5 eV is assigned to N-H which increases in intensity as the reaction progresses which indicates the functionalisation of the surface with hydrogen which enhances over time. The peak at 402.6 eV corresponds to graphitic nitrogen,[8] presumably from the Ensaco carbon powder support.

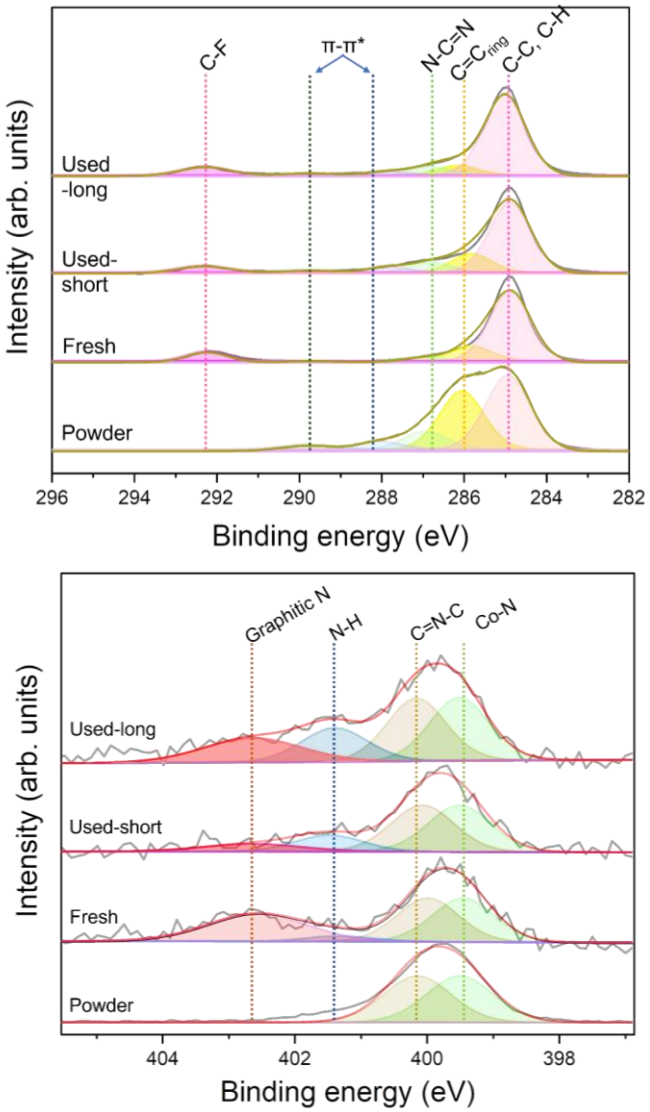

Figure S3. A) C 1s spectra and **B)** N 1s spectra of CoPc GDEs at various stages of the analysis. Spectrum of the CoPc powder is shown for reference.

Scanning Electron Microscopy (SEM) and Energy Dispersive X-ray (EDX)

Fresh vs used cathode with pure water anolyte

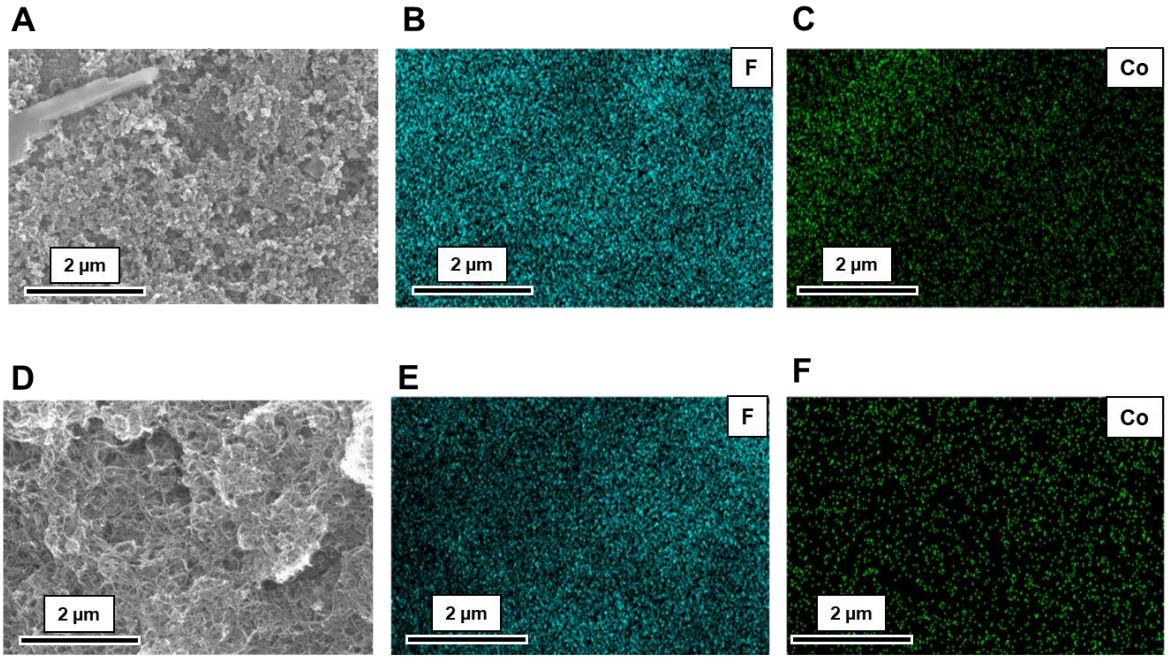

Figure S4. Scanning Electron Microscopy (SEM) and Energy Dispersive X-ray (EDX) mapping of a CoPc/carbon on carbon paper electrode, fresh (A-C), and after 4 h operation (D-F) at 100 mA cm^{-2} with pure water anolyte.

Table S2 Atomic percentages of selected elements from EDX

	% atom			
Sample	F	Co	Na	CO:F
Fresh	90.0	8.1	1.9	0.090
Used short (30 min)	81.5	5.9	12.6	0.072
Used long (4 h)	79.1	5.7	15.2	0.072

Photograph of custom bipolar membrane

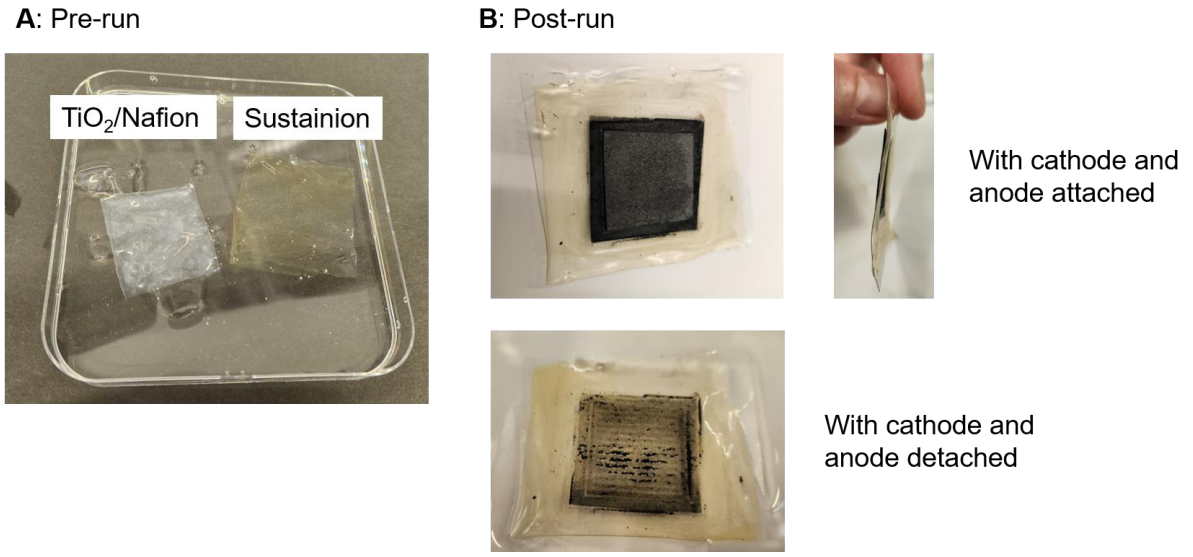

Figure S5. Photographs of **A)** Pre-run TiO_2-loaded Nafion 117 and Sustainion X37-50 membranes and **B)** the assembled Nafion/TiO_2/Sustainion membrane after 3 h operation at 100 mA cm^{-2}.

In our cell configuration (zero-gap, with the membrane directly pressed against the catalyst layer, without any intervening layer) the hydrogen evolution yield is a reasonable proxy for local pH. However, identifying the cause of the different local pH at the cathode is extremely challenging. As the reviewer notes this will be a function of background charge density, water dissociation kinetics, potential co-ion transport, proton transport kinetics, degree of hydration and also it will depend on the degree/nature of the physical contact between the catalyst GDE and the membrane.

In the main text we report water dissociation resistances from ~6-8 Ω cm^2 for studies carried out at room temperature. This is reasonably similar to recent work by Chen et al.[9] who reported WD resistances ranging from ~0.5 to 6.5 Ω cm^2 at 55 °C for similar BPMs, depending on the formulation of the custom BPM (oxide material and loading) and the operating conditions. The differences will be in part at least due to the different temperature as the increased temperature would decrease the WD resistance. Although commercial systems are likely to be run above room temperature here we chose room temperature for a fair comparison to Fumasep, which is not recommended to operate at elevated temperatures.

Changes in various resistances and cathode capacitance during operation

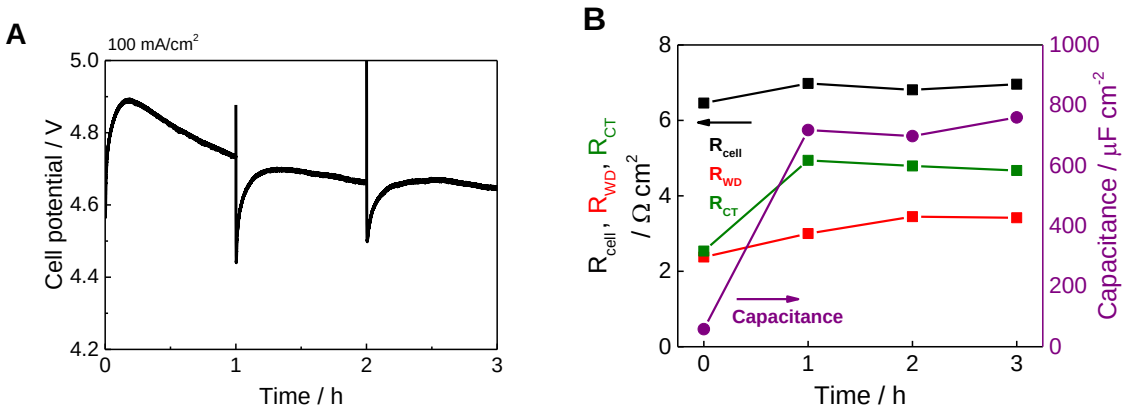

Figure S6. A) Cell voltages at 100 mA cm^{-2}, stopping at each hour to conduct EIS and double-layer capacitance measurements. **B)** The various resistance-area products (left axis): cell resistance (black), water dissociation resistance (red), and charge transfer resistance (green). The cathode double-layer capacitance (purple, right axis). Conditions: cathode CoPc/carbon, anode RuO_2, anolyte pure water, membrane Fumasep FBM.

Effect of adding KCl directly to the CoPc/cathode, while using pure H_2O anolyte

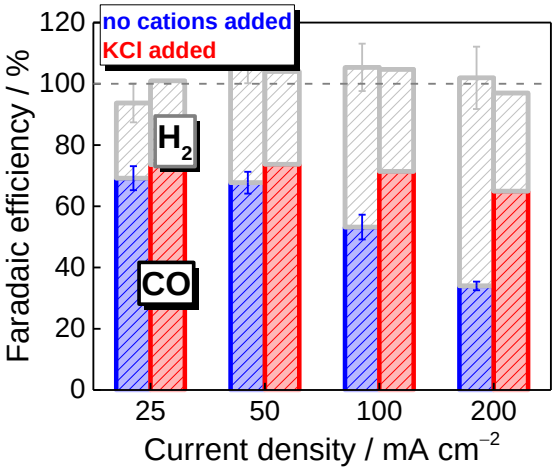

Figure S7. The effect of KCl addition on the Faradaic efficiency, with no added cations (blue, from Figure 2A in the main text), and with KCl added (red). The KCl was added by dropping 0.25 mL of 1 M KCl solution onto the CoPc/carbon cathode (equivalent to 3.7 mg cm^{-2} of KCl loading), leaving to dry, then assembling as usual in the zero-gap cell. Conditions: cathode CoPc/carbon, anode RuO_2, anolyte pure water, membrane Fumasep FBM.

Used cathode with 1 M KOH anolyte

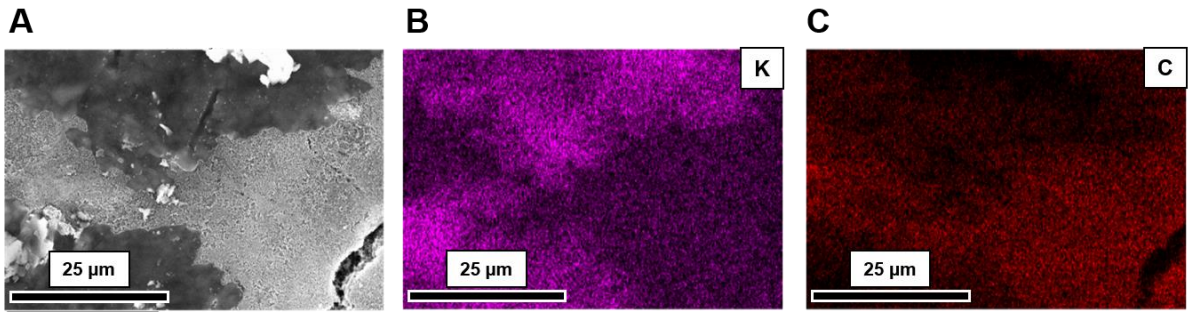

Figure S8. Scanning Electron Microscopy (SEM) and Energy Dispersive X-ray (EDX) mapping of a CoPc/carbon on carbon paper electrode after 44 h operation at 100 mA cm^{-2} with 1 M KOH anolyte.

Stability with 1 M KOH anolyte

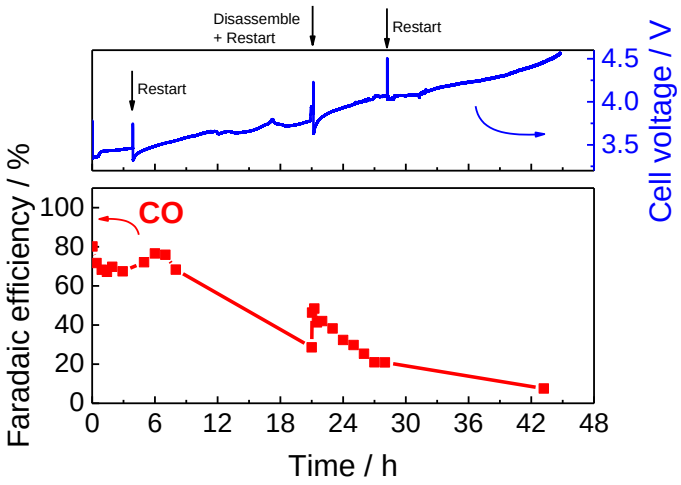

Figure S9. Stability of the cell voltage (top) and CO Faradaic efficiency (bottom), for a CoPc/carbon cathode with 1 M KOH anolyte, at 100 mA cm^{-2}

References

1. Siritanaratkul, B.; Forster, M.; Greenwell, F.; Sharma, P. K.; Yu, E. H.; Cowan, A. J., Zero-Gap Bipolar Membrane Electrolyzer for Carbon Dioxide Reduction Using Acid-Tolerant Molecular Electrocatalysts. *Journal of the American Chemical Society* **2022,** *144* (17), 7551-7556.
2. Blommaert, M. A.; Subramanian, S.; Yang, K.; Smith, W. A.; Vermaas, D. A., High Indirect Energy Consumption in AEM-Based CO2 Electrolyzers Demonstrates the Potential of Bipolar Membranes. *ACS Applied Materials & Interfaces* **2022,** *14* (1), 557-563.
3. Xie, K.; Miao, R. K.; Ozden, A.; Liu, S.; Chen, Z.; Dinh, C.-T.; Huang, J. E.; Xu, Q.; Gabardo, C. M.; Lee, G.; Edwards, J. P.; O'Brien, C. P.; Boettcher, S. W.; Sinton, D.; Sargent, E. H., Bipolar membrane electrolyzers enable high single-pass CO2 electroreduction to multicarbon products. *Nature Communications* **2022,** *13* (1), 3609.
4. Yang, K.; Li, M.; Subramanian, S.; Blommaert, M. A.; Smith, W. A.; Burdyny, T., Cation-Driven Increases of CO2 Utilization in a Bipolar Membrane Electrode Assembly for CO2 Electrolysis. *ACS Energy Letters* **2021,** *6* (12), 4291-4298.
5. Yan, Z.; Hitt, J. L.; Zeng, Z.; Hickner, M. A.; Mallouk, T. E., Improving the efficiency of CO2 electrolysis by using a bipolar membrane with a weak-acid cation exchange layer. *Nature Chemistry* **2021,** *13* (1), 33-40.
6. Salvatore, D. A.; Weekes, D. M.; He, J.; Dettelbach, K. E.; Li, Y. C.; Mallouk, T. E.; Berlinguette, C. P., Electrolysis of Gaseous CO2 to CO in a Flow Cell with a Bipolar Membrane. *ACS Energy Letters* **2018,** *3* (1), 149-154.
7. Schmid, M.; Kaftan, A.; Steinrück, H.-P.; Gottfried, J. M., The electronic structure of cobalt(II) phthalocyanine adsorbed on Ag(111). *Surf. Sci.* **2012,** *606* (11), 945-949.
8. Alwin, E.; Nowicki, W.; Wojcieszak, R.; Zieliński, M.; Pietrowski, M., Elucidating the structure of the graphitic carbon nitride nanomaterials via X-ray photoelectron spectroscopy and X-ray powder diffraction techniques. *Dalton Transactions* **2020,** *49* (36), 12805-12813.
9. Chen, L.; Xu, Q.; Oener, S. Z.; Fabrizio, K.; Boettcher, S. W., Design principles for water dissociation catalysts in high-performance bipolar membranes. *Nature Communications* **2022,** *13* (1), 3846.